RESEARCH ARTICLE

DOI: 10.54926/jnamt.2026.2538

J Nav Architect Mar Technol 2026;228:43-54

Modal Decomposition on the Emergence of High Mean Lift Regimes in 2-DOF Cylinder Forced Motions

Erdem Aktosun

İzmir Katip Çelebi University Faculty of Naval Architecture and Maritime, Department of Shipbuilding and Ocean Engineering, İzmir, Türkiye

To cite this article: E. Aktosun. Modal decomposition on the emergence of high mean lift regimes in 2-DOF cylinder forced motions. *J Nav Architect Mar Technol*. 2026;228:43-54.

Received: 17.12.2025 - **Revision Requested:** 21.01.2026 - **Last Revision Received:** 12.02.2026 - **Accepted:** 04.04.2026 - **Publication Date:** 20.05.2026

Abstract

This study investigates the wake dynamics and mechanisms of mean-lift generation in the two degrees of freedom forced motion of a circular cylinder subjected to combined in-line and cross-flow oscillations. A comprehensive experimental database of 9555 force measurements and 819 Digital Particle Image Velocimetry cases was analyzed using Proper Orthogonal Decomposition. The results show that, under certain motion conditions, a significant mean-lift coefficient arises, which is comparable in magnitude to the oscillatory component. Modal decomposition reveals that while low-mean-lift cases are dominated by two modes that capture approximately 50% of the total flow energy in the first two subspaces, high-mean-lift regimes show increased modal energy dispersion, where the first two subspaces account for approximately 35% of the energy and require three dominant modes for accurate wake reconstruction. These results provide a new physical understanding of coupled forced motion interactions and a foundation for data-driven modeling of high mean-lift regimes in offshore systems.

Keywords: 2-DOF forced motion, POD, wake asymmetry, mean lift coefficient, fluid-structure interactions

1. Introduction

Slender cylindrical structures such as marine risers, subsea pipelines, and mooring lines are critical components of offshore oil, gas, and renewable energy systems. These structures are subjected to ocean currents that trigger complex fluid-structure interactions (FSIs). A primary concern is vortex-induced vibration (VIV), which arises from periodic vortex shedding in the wake of a bluff body. VIV can result in large oscillatory motions, significantly increasing fatigue damage and compromising structural integrity [1-3]. Over recent decades, researchers have focused on predicting VIV, specifically regarding cross-flow and in-line oscillatory responses.

These oscillatory behaviors have several implications. Operationally, they can restrict serviceability and, in severe cases, cause structural failure through accumulated fatigue damage. For offshore structures, VIV impacts are amplified by the combination of harsh environmental conditions and high structural slenderness. Therefore, accurate VIV prediction and modeling are critical for the safe design and reliable operation of deep-water risers, mooring systems, and related infrastructure.

VIV dynamics are nonlinear because the flow strongly interacts with the structural motion. This interaction becomes more complex when motion occurs in both the cross-flow and in-line directions. While earlier works mainly focused

Address for Correspondence: İzmir Katip Çelebi University Faculty of Naval Architecture and Maritime, Department of Shipbuilding and Ocean Engineering, İzmir, Türkiye

E-mail: erdem.aktosun@ikcu.edu.tr

ORCID ID: orcid.org/0000-0002-7391-4060

on one degree of freedom (1-DOF) motion [4], real offshore structures undergo multiple degrees of freedom vibrations. Therefore, 2-DOF systems have shown a more accurate approach to predict VIV [5]. Including in-line motion complicates the vortex shedding process, significantly changing wake patterns and hydrodynamic forces. Studies show that in-line motion shifts the vortex shedding phase and transforms wake structures, sometimes eliminating vortex modes observed in purely transverse oscillations.

An experimental study investigated VIV in elastically mounted cylinders within low-Reynolds-number uniform flows, identifying various wake modes [4]. These modes depend strongly on oscillation amplitude and wavelength. Later experiments by Morse and Williamson [6] expanded this understanding by exploring a wide parameter space of motion frequencies and amplitudes at higher Reynolds numbers. They observed a transitional vortex mode characterized by two vortex pairs per shedding cycle, where the second pair is weaker than the first. This work highlighted the necessity of mapping vortex modes and hydrodynamic forces across diverse motion conditions to fully capture VIV complexity.

When in-line motion is combined with cross-flow oscillations, additional wake modes emerge. Research by Morse and Williamson [7] showed that harmonic in-line motion significantly alters wake structures during transverse oscillation. Free vibration studies [8] confirmed these results and identified complex vortex patterns typically associated with large cross-flow amplitudes in low-mass ratio systems. The complexity increases when the cylinder follows the figure-eight trajectories inherent in 2-DOF free vibrations. Experiments by Aronsen [9] and subsequent computational studies by [10,11] revealed that clockwise and counter-clockwise trajectories produce different wake asymmetries. These results indicate that combined motions are not a simple superposition of independent effects but represent a fundamentally coupled nonlinear system.

Understanding these complex wake dynamics is important for fatigue life estimation and structural integrity assessments. However, modeling VIV in long flexible structures remains challenging due to nonlinear FSIs and varying Reynolds numbers. While direct numerical and large-eddy simulations provide fundamental insights, their application to full-scale structures is computationally demanding. Therefore, semi-empirical approaches, which couple simplified structural models with experimentally derived hydrodynamic coefficients, have emerged as a practical engineering alternative.

Research by Chaplin et al. [12] showed that semi-empirical models using experimental force data can predict cross-flow motions in long flexible structures more reliably than high-resolution simulations under certain conditions. However, [13-15] noted that hydrodynamic forces during combined cross-flow and in-line motion differ significantly from those during 1-DOF oscillations. These results emphasize the necessity of dedicated experimental datasets capturing the coupled nature of VIV. Constructing such databases is challenging due to the vast parameter space required, including variations in amplitude ratio, frequency ratio, phase difference, and trajectory pattern.

Recent studies have shown significant mean lift forces during certain forced combined motions [16]. These forces can be comparable in magnitude to oscillatory lift, suggesting a clear asymmetry in the wake structure. Such asymmetry has important implications for long, flexible structures, potentially leading to mean deflections or kiting perpendicular to the flow. These phenomena present a new challenge in understanding the physics governing asymmetric wake formation. Identifying the conditions that trigger these large mean lift forces and correlating them with specific wake modes remains a critical research question with considerable practical relevance.

To address the complexity of wake dynamics in combined motion systems, advanced data-driven methods have been employed to extract dominant flow features and characterize the time evolution of vortical structures. Among these, Proper Orthogonal Decomposition (POD) has emerged as a powerful technique for analyzing large experimental and computational datasets. POD decomposes flow fields into orthogonal modes ranked by energy content, providing a systematic way to identify the structures most critical to the overall dynamics. Unlike traditional phase-averaging techniques, which assume periodicity and require phase alignment, POD captures both coherent and intermittent features. This makes it particularly suitable for analyzing the nonlinear and potentially chaotic wake patterns in combined-motion VIV [17].

Previous studies [17-20] have utilized POD and related modal decomposition techniques to identify the dominant flow structures associated with different wake modes and to correlate these modes with the structural responses of a circular cylinder undergoing VIV. Similarly, [21] applied POD to analyze the nonlinear responses of flexible cylinders exhibiting hysteresis and mode transitions. These works highlight POD's potential not only as a diagnostic tool but also as a foundation for developing reduced-order models (ROMs) for predictive purposes.

In the context of large mean forces and asymmetric wakes, POD offers a promising approach for identifying the spatial modes responsible for asymmetry and linking them to

specific motion parameters. Decomposing the flow field to examine the contribution of individual modes to mean lift generation clarifies how combined cross-flow and in-line motions produce wake asymmetry. Such insights are essential for advancing semi-empirical models to include mean force effects and for improving the resolution of VIV prediction frameworks.

While previous studies [16,22,23] provided extensive force mappings, a fundamental research gap remains regarding the physical modal interactions that trigger sustained wake asymmetry**.** This study fills that gap by using POD to isolate the specific coherent structures responsible for high mean-lift generation, which were not detailed in the earlier studies. A mean lift coefficient map was created from the database [22] to explore the complex dynamics of combined in-line and cross-flow vibrations of a circular cylinder under forced motion. In this study, the primary objective is to isolate the coherent structures responsible for the transition between low and high mean-lift regimes. By applying POD to representative cases, we characterize the phase-dependent vortex shedding that triggers the kiting effect, a phenomenon in which sustained hydrodynamic lift causes significant mean structural deflection. This focused analysis provides the physical understandings necessary to bridge the gap between observed force responses and predictive modeling for 2-DOF VIV systems.

2. Materials and Methods

2.1. Flow Visualization Experiment

Experiments were conducted in the flow tank at the University of Rhode Island's Ocean Engineering Department [24]. The tank measures 1.05 m by 0.75 m by 2.80 m and can generate flow speeds up to 1.3 m/s. A test cylinder was mounted on a force sensor and secured to an aluminum frame spanning the tank width for stability, positioned 3.5 mm above the bottom to avoid tip vortices. Wake structures were recorded using a Phantom V10 high-speed camera at 250 Hz with 2400×540-pixel resolution and a lateral green laser sheet mounted on a motorized frame, shown in Figure 1. The carbon cylinder had a diameter of 3.85 cm, a submerged span of 57.25 cm, and a mass of 0.268 kg. Tests were performed at a Reynolds number of 7620 under prescribed sinusoidal cross-flow and in-line motions (Equation 1).

$$y = \frac{A_y}{D}\sin(\omega t) \;\&\; x = \frac{A_x}{D}\sin(2\omega t + \theta) \qquad (1)$$

Where y and x are normalized motions, $A_y^* = A_y/D$ and $A_x^* = A_x/D$ are the cross-flow and in-line amplitudes ω, is the motion frequency and, θ is the phase difference between cross-flow and in-line motions.

A Phantom V10 high-speed camera and a laser system were employed for Digital Particle Image Velocimetry (DPIV) measurements to capture the wake dynamics around the test cylinder. The initially collimated laser beam was converted into a thin sheet using optical elements, allowing planar illumination of multiple particles simultaneously. This laser sheet was carefully positioned within the fluid to illuminate the region of interest for flow visualization. Motion parameters were systematically varied during the experiments: in-line oscillation amplitude ranged from 0.1 to 0.3, cross-flow amplitude from 0.1 to 1.6, reduced velocity from 5 to 7, and phase angle from -180° to 180° in 30° increments. A total of 819 test cases were performed, forming a comprehensive experimental database. Variations in phase angle produced distinct orbital trajectories of the cylinder, with θ=0° corresponding to a counter-clockwise figure-eight path, consistent with previous studies [16,22,24].

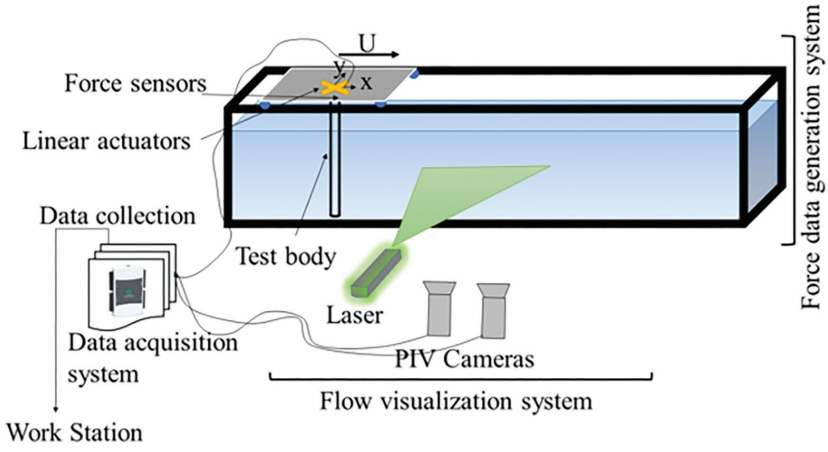

Figure 1. Schematic of the experimental setup at the flow tank, showing the integrated force data generation system (linear actuators and force sensors) and the flow visualization system (PIV cameras and laser sheet orientation)

PIV: Particle Image Velocimetry

2.2. Modal Decomposition Method

Vortex patterns behind an oscillating circular cylinder were investigated using flow visualization experiments and POD analysis, as explained in [23]. By varying motion parameters and applying the POD analysis based on the formulation in [23], the study identified and correlated wake structures with experimental data to improve the prediction of vortex behavior and enhance the understanding of FSIs. The modal decomposition approach, following [23], was used to analyze wake patterns associated with both low and high mean lift forces, as identified from a comprehensive force and wake database [16,22,24]. In this approach, let us consider that the function $\Gamma(X,t)$ denotes the vorticity field as a function of both spatial position X along the spanwise direction and time, t. The temporal evolution of this quantity can be described through a modal representation in which the flow field is expressed as a linear combination of orthogonal spatial modes. Mathematically, this can be formulated as (Equation 2):

$$\Gamma(X,t) \approx \sum_{k=1}^{N} a_k(t)\,\Phi_k(X) \qquad (2)$$

In this formulation, $\Phi_k(X)$ corresponds to the spatial structure (or shape function) of the k^{th} mode, while $a_k(t)$ represents its associated time-dependent coefficient or amplitude. The index enumerates the modes, and defines the number of modes retained in the modal expansion. This decomposition provides a compact representation of the system's dynamics by isolating dominant flow patterns from the full data field.

To obtain these modal structures from empirical or simulated flow data, Singular Value Decomposition (SVD) can be applied to the vorticity matrix $\Gamma(X,t)$. The decomposition takes the following canonical form: $\Gamma(X,t) = U\Sigma V^{T}$. Here, U is an orthogonal matrix of dimension MxM containing the spatial modes, commonly referred to as Proper Orthogonal Modes (POMs). The matrix $V(NxN)$ encodes the temporal evolution of the corresponding modes, while $\Sigma(MxN)$ is a diagonal matrix whose elements, the singular values σ_i, quantify the energy contribution of each mode to the overall dynamics.

Through this POD framework, the original high-dimensional dataset can be approximated using only a subset of modes that capture the most energetic flow features. The data can thus be reconstructed with reduced dimensionality by retaining the leading singular values, such that $r < N$. The resulting truncated representation preserves the dominant physical characteristics of the system while significantly reducing computational cost.

The accuracy and physical relevance of this ROM depend strongly on the singular value spectrum in Σ. Each singular value reflects the portion of total kinetic or vorticity energy contained within its associated mode. The fractional energy contribution of the k^{th} mode can therefore be defined as (Equation 3):

$$E_k = \frac{\sigma_k}{\sum_{i=1}^{N}\sigma_i} \qquad (3)$$

This energy ratio provides a quantitative measure of the significance of each mode in describing the system's overall motion. Typically, only a small number of dominant modes are required to capture the essential dynamics, while higher-order modes primarily represent small-scale or noise-like structures.

The POD was implemented using the snapshot method via SVD on a dataset of 793 DPIV realizations. To isolate fluctuating coherent structures, the vorticity field was first centered by subtracting the ensemble mean from each snapshot. The spatial domain consisted of a 142x111 grid, with a sampling frequency of 250 Hz. To ensure spectral accuracy, a Hamming window was applied to the modal coefficients to minimize spectral leakage during frequency estimation. Finally, the POD reconstruction served as a physics-based filter; by retaining only the dominant modes and discarding higher-order ones, high-frequency experimental noise was removed while preserving the physically significant vortex dynamics.

The selection of dominant POD modes is based on cumulative energy contribution. In low mean-lift regimes, the first two subspaces capture approximately 50% of the total fluctuation energy, representing periodic shedding. For high mean-lift cases, a third mode is included (approximately 35% for two subspaces) to accurately reconstruct the biased vortex formation. Modes beyond the third represent incoherent noise and were excluded to focus on the large-scale structures driving mean-lift forces.

3. Results and Discussion

This section presents the flow visualization and POD results for wake structures behind a circular cylinder undergoing combined motions under low and high mean lift force conditions. The objective is to identify dominant flow features and correlate motion parameters with wake asymmetry and vortex dynamics. By systematically varying amplitudes, reduced velocity, and phase, large mean lift forces were observed at specific parameters. POD allows the decomposition of complex vorticity fields into energy-ranked spatial modes, facilitating a clear observation of dominant coherent structures. The following sections discuss wake pattern evolution, the energetic contribution of leading modes, and their relationship to asymmetric flow features.

Analysis of the decomposed hydrodynamic forces reveals several notable characteristics of the coupled motion. A key

finding is the significant variability of the effective cross-flow added mass coefficient across the tested parameters, aligning with results for freely vibrating cylinders [16]. In contrast, the in-line added mass coefficient remains relatively stable at low motion amplitudes typical of free vibration. For most cases, this coefficient is negative and nearly constant. These results suggest that variations in the effective natural frequency of systems undergoing simultaneous oscillations are primarily driven by the cross-flow component rather than the in-line response [16,22].

Considering excitation forces in phase with cylinder velocity provides further insights into in-line motion. While excitation in 1-DOF transverse systems is characterized by the velocity-aligned force component, this simplification is insufficient for coupled systems. Because energy is exchanged dynamically between in-line and cross-flow components, the total energy transfer must be considered. Therefore, a total power coefficient was introduced based on the combined forces in phase with both motion directions [24,25]. Results show that in-line motion expands the region of positive energy transfer from the fluid to the structure, thereby enhancing oscillation amplitudes. This aligns with free-vibration studies where coupled motion amplifies the system's dynamic response.

3.1. High Mean-Lift regimes in 2-DOF Forced Motions

It is well established that VIV can increase the mean drag force experienced by a cylinder. However, an unexpected result from the present investigation is the appearance of a substantial mean lift coefficient under specific motion combinations. In some cases, the mean lift reaches values exceeding 1.0, comparable to the amplitude of the fluctuating lift coefficient observed during certain oscillations. Figure 2 presents contour maps of the mean lift coefficient for two selected in-line motion amplitudes of 0.2 and 0.5 when cross-flow amplitude is fixed at 0.35. These plots illustrate the influence of reduced velocity (radial coordinate) and the phase difference between motions (angular coordinate). The results demonstrate that large mean lift coefficients emerge only due to the cylinder's forced motion, indicating significant wake asymmetry. Although asymmetric wakes occur under purely cross-flow forcing [4], the magnitudes observed here suggest that such asymmetry could induce substantial mean lift on elongated or flexible structures. Detailed wake visualizations for high-mean-lift cases are presented below to further explore this phenomenon.

To investigate these dynamics, we compared the wake structures of two distinct cases: one with a low mean lift force and another with a high mean lift force. POD was then applied to analyze the modal decomposition of each wake. This analysis revealed that high mean lift cases show significantly more complex and disorganized wake topologies than low mean lift cases.

Figures 3 and 4 present the wake structures behind the cylinder for selected low and high mean lift conditions. In Figure 3 (low mean lift), the wake exhibits a highly coherent vortex shedding pattern, maintaining periodicity and structural integrity several diameters downstream. Correspondingly, the time histories of non-dimensional lift and drag forces show periodic oscillations with stable amplitudes and frequencies. The presence of a small, nonzero mean lift component suggests a weak but persistent wake asymmetry that remains stable throughout the observation period.

In contrast, Figure 4 shows a flow field with a more complex and messier vortex formation in the wake. The vorticity contours indicate a breakdown of symmetry with vortex cores appearing diffuse and occasionally merging as they move downstream. Such irregularities and complexities are accompanied by stronger fluctuations in both lift and drag force with potential evidence of amplitude modulation and phase shift. The variation in the mean lift level and sign between Figures 3 and 4 implies that the existing wake asymmetry may have reversed or altered due to differences in the initial conditions or the phase relationship between in-line and cross-flow motion. This interpretation aligns with observations from previous studies that report small variations in reduced velocity or phase can lead to distinct asymmetric wake states characterized by opposite signs of mean lift [26,27].

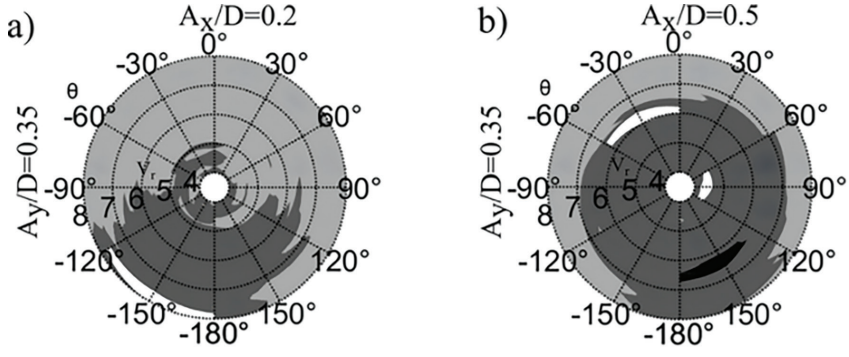

Figure 2. Contour maps of the mean lift coefficient as a function of reduced velocity and phase angle for two cases: (a) Small in-line amplitude (A_y/D=0.35, A_x/D =0.2) and (b) High in-line amplitude (A_y/D=0.35, A_x/D=0.5). The color scale highlights are high mean lift regimes at specific phases.

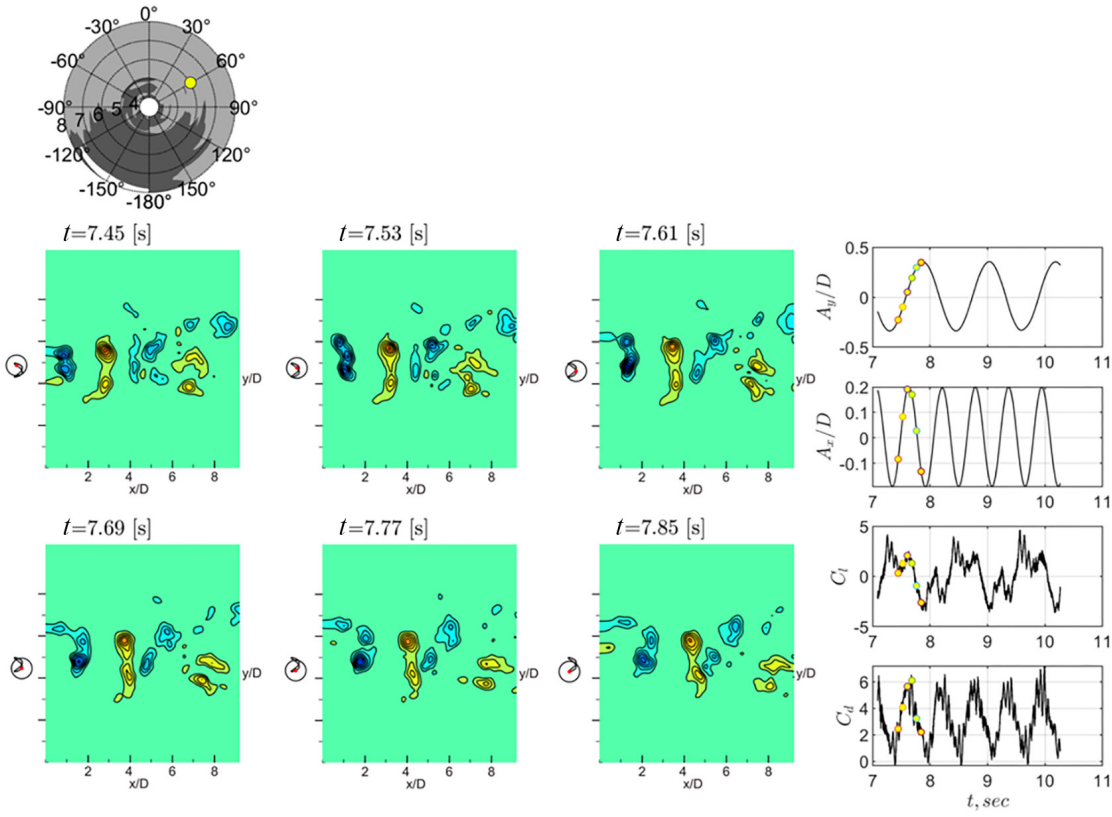

Figure 3. Flow visualization and force response for a low mean-lift case (A_y/D=0.35, A_x/D=0.2, V_r=6, and θ=60°). The panels show instantaneous vorticity across one cycle highlighting clear vortex shedding pattern.

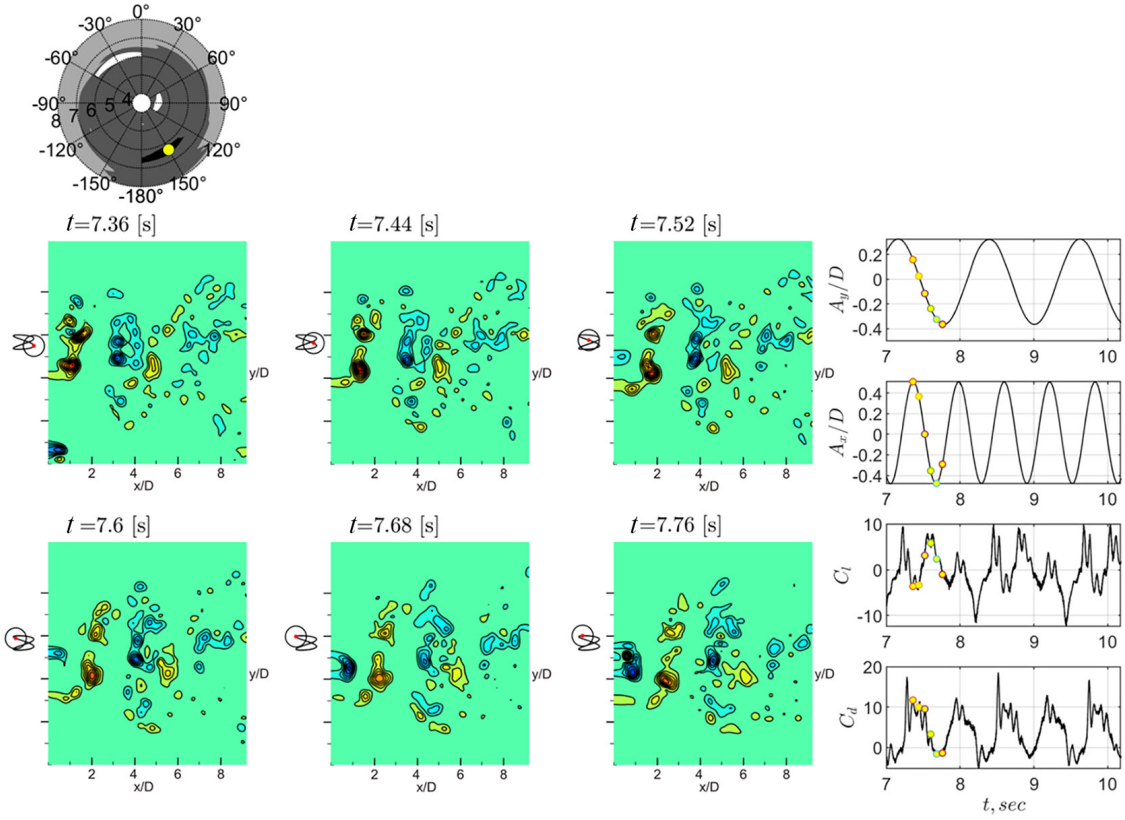

Figure 4. Flow visualization and force response for a high mean-lift case (A_y/D=0.35, A_x/D=0.5, V_r=6.4, and θ=150°). The broken symmetry in the vortex formation leads to a substantial mean lift component comparable to the oscillatory amplitude.

3.2. Modal Decomposition Results

Two representative cases were selected from the forced VIV database to evaluate POD's capability in capturing coherent structures at different mean lift levels. The low-mean lift is defined by $A_y/D = 0.35$, $A_x/D = 0.2$, $V_r = 6$, and $\theta = 60°$, while the high-mean lift is characterized by $A_y/D = 0.35$, $A_x/D = 0.5$, $V_r = 6.4$, and $\theta = 150°$. Analysis focused on the first two dominant subspaces, with particular emphasis on the primary mode. A third case with larger in-line motion and moderate variations in reduced velocity and phase was also examined; however, significant noise and nonlinear FSIs made the identification of a dominant mode uncertain. This suggests that further investigation is required to better resolve the complex coupling and improve modal decomposition accuracy.

Figure 5a presents the POD analysis for twelve modes under the low mean lift condition. The first two POMs exhibit well-defined, coherent spatial structures that capture approximately 50% of the total energy, indicating a dominant and repeatable wake pattern. Conversely, POM3 through POM6 display distinct characteristics, representing secondary flow features. Beyond these six modes, the spatial structures become progressively disorganized, suggesting that higher-order subspaces primarily represent small-scale fluctuations rather than coherent dynamics. Importantly, the POMs must be viewed alongside their temporal coefficients to fully reveal the underlying evolution of these structures.

Furthermore, Figure 5b reveals another energy grouping encompassing subspaces 3 through 6. Examination of their corresponding POMs, Proper Orthogonal Coefficients, and Proper Orthogonal Values indicates that these modes share comparable spatial and temporal behavior, implying that their combination forms a secondary coherent mode representing a distinct wake pattern. Modes beyond the sixth subspace exhibit no clear structure and are therefore interpreted as noise or residual turbulence in the wake.Although twelve subspace dimensions (six modes) are presented for completeness, the analysis indicates that only two distinct coherent wake patterns exist, with one clearly dominating the overall flow dynamics.

Figure 6 analyzes the high mean lift regime where the wake shows increased complexity. The energy distribution (Figure 6b) indicates that a third mode is necessary to represent the enhanced asymmetry, with the he first two subspaces capturing approximately 35% of the total energy. The first two POMs share similar temporal evolutions and frequency components (Figures 6c and 6d), signifying that their combination represents the primary vortex-shedding mode. This dominant frequency aligns with the wake dynamics observed in the vorticity contours (Figure 6a). Conversely, modes beyond the third mode show no discernible patterns and likely contribute to observed wake noise. Higher-order modes (subspaces>6) exhibit irregular spatial structures and minimal energy, representing small-scale turbulence or residual irregularities. Their fluctuating temporal behavior and broad frequency spectra confirm that these modes capture high-frequency, low-energy disturbances rather than coherent shedding.

Figure 7 compares raw DPIV vorticity fields (left) with POD reconstructions (right) for two distinct mean lift cases. Figure 7a represents the low mean lift condition ($A_y/D = 0.35$, $A_x/D = 0.2$, $V_r = 6$, and $\theta = 60°$), while Figure 7b captures the high mean lift condition ($A_y/D = 0.35$, $A_x/D = 0.5$, $V_r = 6.4$, and $\theta = 150°$). Instantaneous snapshots are shown at four non-dimensional times (t/T=0.2, 0.5, 0.8, 1.2), covering a full oscillation cycle. For the low mean lift case, a reconstruction using only the first two POD modes effectively captures the dominant vortices and their phase-dependent evolution, successfully filtering out fine-scale experimental noise. In contrast, the high mean lift case exhibits a more complex, asymmetric wake with intense vortex interactions. Here, a three-mode reconstruction is required to accurately reproduce the dominant vortex cores and their deformation while significantly reducing the random fluctuations visible in the raw DPIV data.

Quantitative comparisons reveal that the high mean-lift regime is defined by a distinct shift in modal energy and spectral power. While low-lift cases are dominated by symmetric shedding captured by the first two modes, the high-lift case requires a three-mode reconstruction, as the first two subspaces account for only approximately 35% of the cumulative energy required to resolve wake asymmetry. Specifically, the energy contribution of Mode 3 increases significantly in high-lift cases, representing the physical spatial bias or "kiting" of the wake. Furthermore, spectral analysis shows that the peak power magnitude of these primary modes is substantially higher in the high-lift regime. This confirms that increased mean lift results from more energetic, phase-locked coherent structures rather than a simple spatial displacement of the wake.

The transition to wake asymmetry is quantitatively evidenced by the emergence of a high mean lift coefficient that reaches values exceeding 1.0, effectively matching the magnitude of the oscillatory lift component. POD analysis further quantifies this behavior through modal energy distribution: while low-mean-lift cases are characterized by two dominant energetic modes that capture over 50% of the total flow energy, high-mean-lift regimes exhibit increased modal energy dispersion where the two subspaces account for approximately 35% of the total energy and require three dominant modes for accurate wake reconstruction.

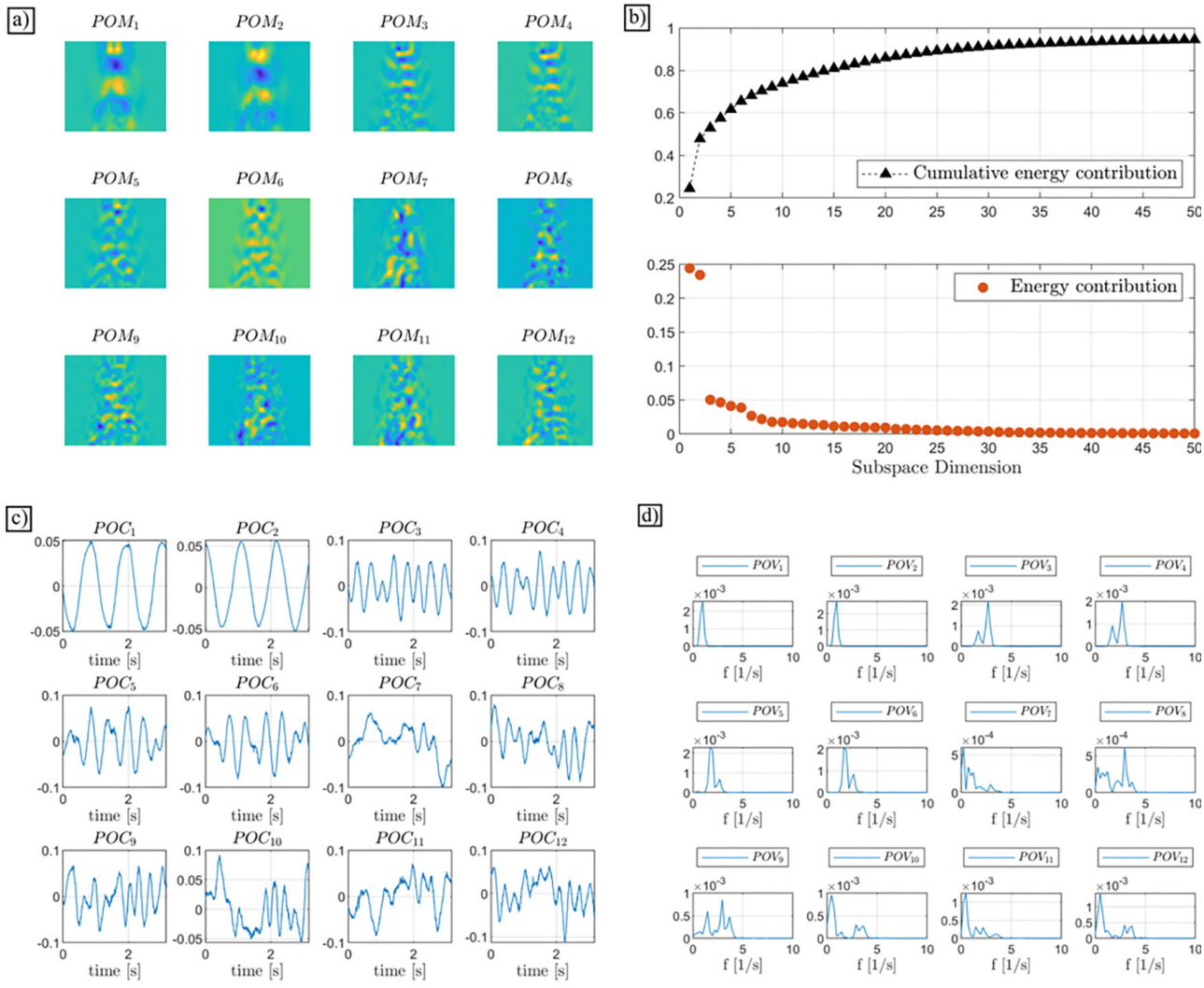

Figure 5. POD analysis for the low mean-lift case (A_y/D=0.35, A_x/D=0.2, V_r=6, θ=60°): (**a**) The first 12 spatial modes (POMs), (**b**) cumulative energy showing that the first two modes dominate, (**c**) temporal coefficients (POCs), and (**d**) frequency spectra (POVs) of the leading modes.

3.3. Discussion

This study shows that 2-DOF forced-motion VIV experiments provide a more comprehensive and physically representative description of FSI than traditional 1-DOF models. Building on the foundational force and wake database of [16,23], this study uniquely implements POD to systematically isolate the coherent structures responsible for mean-lift generation. Unlike traditional phase-averaging methods used in previous studies, our POD-based approach enables the identification of specific energetic modes that drive wake asymmetry even in the presence of experimental noise. While prior studies have established fundamental wake modes through 1-DOF studies [7,28] or sparser 2-DOF measurements [14,15], this study was based on a high-resolution 2-DOF experimental database. Specifically, we expanded the parameter space to include 9555 force measurements and 819 DPIV cases. This density of data allows for the first comprehensive mapping of the high-mean-lift regime, which remained largely unresolved in lower-resolution datasets.

Comparisons with previously reported free-vibration and forced-motion results show strong agreement in wake branches and hydrodynamic force trends [8,13,15,22]. In particular, the broad variation observed in the cross-flow added mass coefficient is consistent with free-vibration studies [13], confirming the reliability of the measurements. More significantly, the present results clearly identify a high mean lift regime, where the mean lift coefficient reaches values comparable to the oscillatory lift component for specific combinations of motion parameters. Flow visualization and POD analysis indicate that this regime is associated with persistent wake asymmetry, consistent with earlier observations in [16].

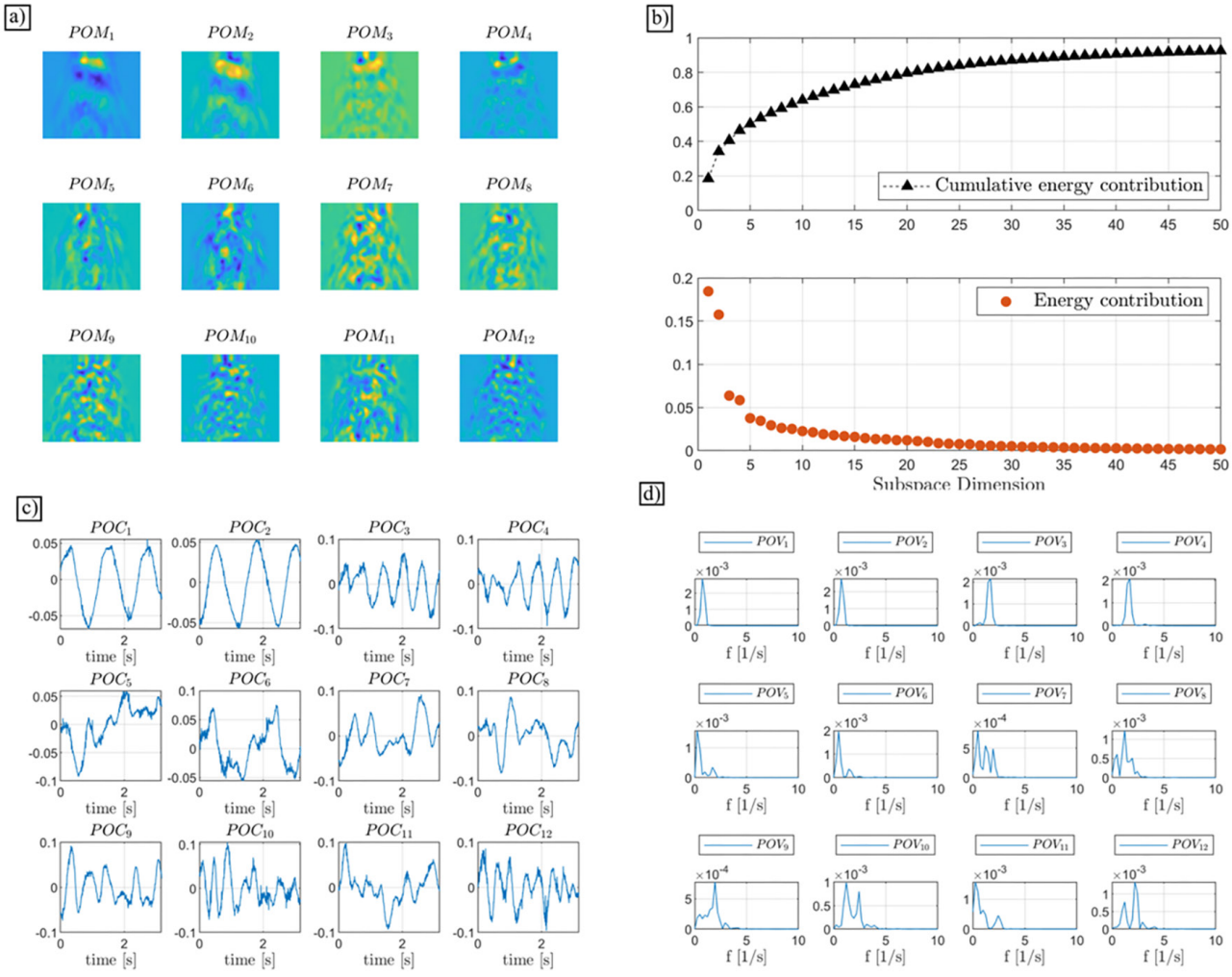

Figure 6. POD analysis for the high mean-lift case (A_y/D=0.35, A_x/D=0.5, V_r=6.4, θ=150°): Increased complexity in the spatial modes and higher energy dispersion across the spectrum compared to the low-lift regime.

Modal decomposition shows that low mean lift cases are dominated by two energetic POD modes, corresponding to relatively symmetric and periodic wake structures. In contrast, high mean lift cases require three dominant modes to accurately reconstruct the wake, reflecting increased asymmetry and nonlinear vortex interactions. Despite this complexity, POD effectively captures the dominant coherent structures while filtering noise, as demonstrated by the reconstructed wake fields.

The presence of sustained mean lift forces has important implications for offshore risers and slender marine structures, potentially leading to kiting-like behavior even for bare cylinders [16]. While the present experiments were conducted at a constant Reynolds number [8,29], Reynolds number effects remain an important limitation, as wake asymmetry and force characteristics may vary significantly [30-32]. This study utilized a constant Reynolds number to align with previous benchmarks. However, Reynolds number is a critical parameter that may influence the high mean-lift regions identified in this database. It remains an open question how varying Reynolds number affects the boundaries of these regions or the underlying vortex formation in the wake. Specifically, higher Reynolds numbers could modify the wake asymmetry that drives these forces. While our results provide a fundamental map of the mean-lift regime, testing at higher Reynolds number is necessary to determine if these 'kiting' forces persist or evolve in the conditions with varying Reynolds numbers typical of full-scale offshore applications.

The presence of a strong mean lift force implies a significant and persistent asymmetry in the wake. While such asymmetries have been observed for forced cross-flow motion [6], the lift magnitudes measured here are comparable to coefficients associated with true lifting

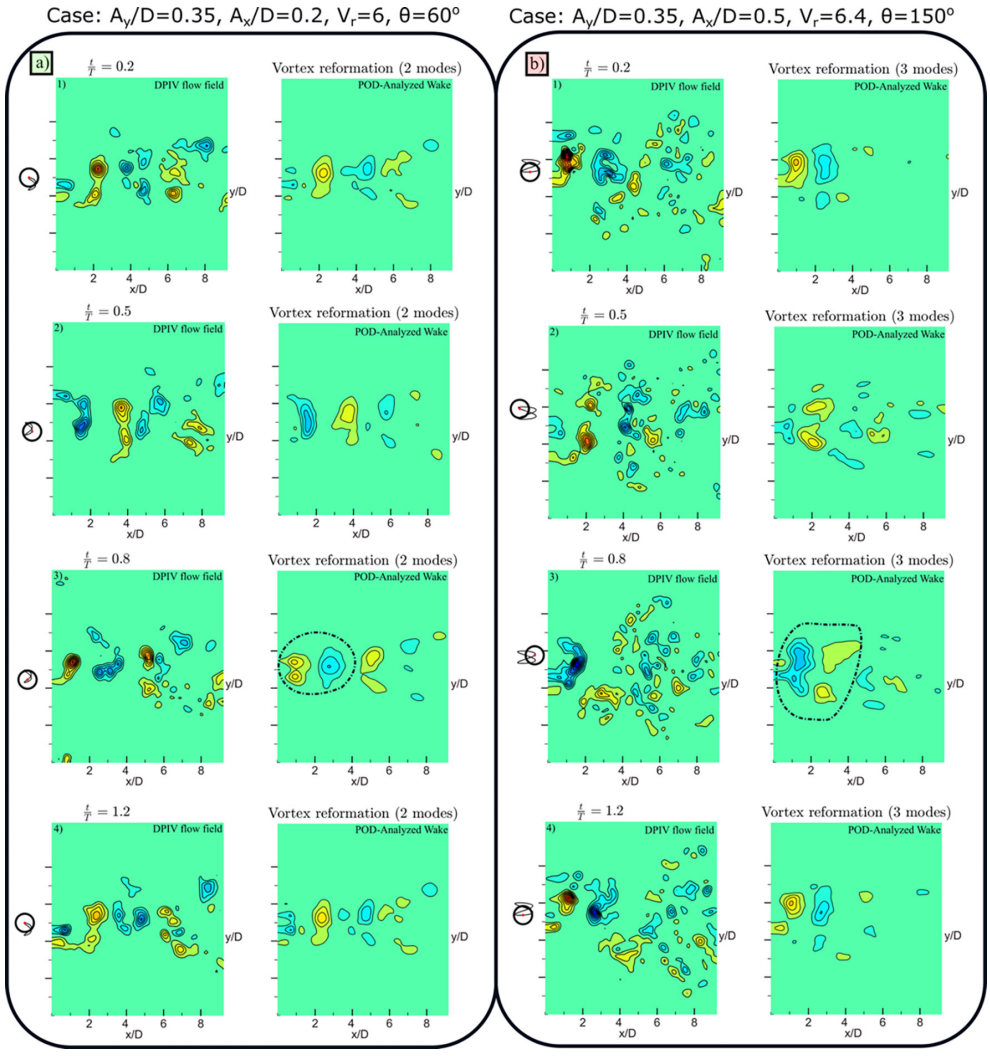

Figure 7. **a**) Comparative snapshots of raw DPIV vorticity and POD reconstructions at non-dimensional times. **a**) Reconstruction using 2 modes for low mean lift; (**b**) Reconstruction using 3 modes for high mean lift, illustrating how POD captures the essential asymmetric wake structures while filtering experimental noise.

surfaces. Importantly, this mechanism defines the mean lift region within our database. We observed that the mean lift does not switch signs when experiments are repeated [16], suggesting that the specific asymmetry is a stable feature of the forming wake structure. Furthermore, experiments with similar motion parameters exhibit consistent behaviors, where a significant mean lift of a specific sign is observed across multiple cases. On long, slender structures like marine risers, this hydrodynamic state can lead to "kiting" or mean deflections perpendicular to the flow. In the case of a riser undergoing VIV, these motion conditions would result in a side deflection dependent on the structural stiffness, making the characterization of this asymmetric regime critical for predicting the equilibrium of flexible structures.

Future numerical investigations [33], combined with data-driven approaches such as Artificial Neural Network-based force modeling [25,34] and complementary modal techniques including D Dynamic Mode Decomposition (DMD) [35] and Smooth Orthogonal Decomposition (SOD) [21,36] offer promising pathways to generalize these results and enhance predictive VIV frameworks.

4. Conclusion

This study presents a detailed modal decomposition analysis of wake structures generated by a circular cylinder undergoing 2-DOF forced motion in uniform flow. Using an extensive DPIV experimental database, POD effectively identifies the dominant coherent modes responsible for wake asymmetry and high mean lift generation. The analysis shows that cases with high mean lift show complex, asymmetric vortex interactions and increased modal energy dispersion, whereas low mean-lift conditions are

characterized by clear and symmetric wake patterns. The results confirm that the emergence of large mean lift forces is closely associated with complexity and nonlinear coupling between in-line and cross-flow motions. By reconstructing wake fields using a limited number of energetic modes, the study highlights POD's capability as a robust diagnostic tool for noise reduction and ROM of complex VIV flows. These results advance the physical understanding of asymmetric wake dynamics and provide a valuable experimental basis for improving predictive models in offshore engineering applications, including flexible risers, cables, and tethered systems operating in oscillatory flow environments.

Footnotes

Financial Disclosure: The author declared that this study received no financial support.

References

[1] C. H. K. Williamson, and R. Govardhan, "Vortex-induced vibrations," *Annual Review of Fluid Mechanics,* vol. 36, no. 1, pp. 413-455, Jan 2004.

[2] T. Sarpkaya, "Vortex-induced oscillations: a selective review," *Journal of Applied Mechanics,* vol. 46, no. 2, pp. 241-258, Jun 1979.

[3] M. S. Triantafyllou, R. Bourguet, J. Dahl, and Y. Modarres-Sadeghi, "Vortex-induced vibrations," in *Springer Handbook of Ocean Engineering*, Cham: Springer International Publishing, 2016, pp. 819-850.

[4] C. H. K. Williamson, and A. Roshko, "Vortex formation in the wake of an oscillating cylinder," *Journal of Fluids and Structures,* vol. 2, no. 4, pp. 355-381, Jul 1988.

[5] P. W. Bearman, "Understanding and predicting vortex-induced vibrations," *Journal of Fluid Mechanics,* vol. 634, pp. 1-4, Aug 2009.

[6] T. L. Morse, and C. H. K. Williamson, "Prediction of vortex-induced vibration response by employing controlled motion," *Journal of Fluid Mechanics,* vol. 634, pp. 5-39, Sep 2009.

[7] T. L. Morse and C. H. K. Williamson, "Fluid forcing, wake modes, and transitions for a cylinder undergoing controlled oscillations," *Journal of Fluids and Structures,* vol. 25, no. 4, pp. 697-712, May 2009.

[8] N. Jauvtis, and C. H. K. Williamson, "The effect of two degrees of freedom on vortex-induced vibration at low mass and damping," *Journal of Fluid Mechanics*, vol. 509, pp. 23-62, Jun 2004.

[9] K. H. Aronsen, "An experimental investigation of in-line and combined in-line and cross-flow vortex induced vibrations," Norwegian University of Science and Technologhy, 2007.

[10] S. Peppa, L. Kaiktsis, and G. S. Triantafyllou, "Numerical simulation of three-dimensional flow past a cylinder oscillating at the strouhal frequency," *Journal of Pressure Vessel Technology,* vol. 137, no. 1, 011302, Feb 2015.

[11] S. Peppa, L. Kaiktsis, and G. S. Triantafyllou, "Hydrodynamic forces and flow structures in flow past a cylinder forced to vibrate transversely and inline to a steady flow," *Journal of Offshore Mechanics and Arctic Engineering,* vol. 138, no. 1, 011803, Feb 2016.

[12] J. R. Chaplin *et al.*, "Blind predictions of laboratory measurements of vortex-induced vibrations of a tension riser," *Journal of Fluids and Structures,* vol. 21, no. 1, pp. 25-40, Nov 2005.

[13] J. M. Dahl, F. S. Hover, and M. S. Triantafyllou, "Two-degree-of-freedom vortex-induced vibrations using a force assisted apparatus," *Journal of Fluids and Structures,* vol. 22, no. 6-7, pp. 807-818, Aug 2006.

[14] J. M. Dahl, F. S. Hover, M. S. Triantafyllou, S. Dong, and G. E. Karniadakis, "Resonant Vibrations of Bluff Bodies Cause Multivortex Shedding and High Frequency Forces," *Physical Review Letters,* vol. 99, no. 14, 144503, Oct 2007.

[15] H. Zheng, J. M. Dahl, Y. Modarres-Sadeghi, and M. S. Triantafyllou, "Coupled inline-cross flow VIV hydrodynamic coefficients database," in *International Conference on Offshore Mechanics and Arctic Engineering Proceedings Series Volume 2: CFD and VIV*, Jun 2014.

[16] E. Aktosun, and J. M. Dahl, "Experimental force database from controlled in-line and cross flow cylinder motion," in *the 28th International Ocean and Polar Engineering Conference*, 2018. [Online]. Available: https://onepetro.org/ISOPEIOPEC/proceedings-abstract/ISOPE18/All-ISOPE18/ISOPE-I-18-547/20713

[17] G. Riches, R. Martinuzzi, and C. Morton, "Proper orthogonal decomposition analysis of a circular cylinder undergoing vortex-induced vibrations," *Physics of Fluids*, vol. 30, no. 10, 105103, Oct 2018.

[18] D. Deep, A. Sahasranaman, and S. Senthilkumar, "POD analysis of the wake behind a circular cylinder with splitter plate," *European Journal of Mechanics - B/Fluids*, vol. 93, pp. 1-12, May-Jun 2022.

[19] Z. Sun, D. Chen, M. Zhang, S. Zhang, and L. Zou, "The pressure mode decomposition analysis of circular cylinder under stationary and VIV conditions," *Ocean Engineering,* vol. 310, 118711, 2024.

[20] H. Jiang and S. Cao, "Balanced proper-orthogonal-decomposition-based feedback control of vortex-induced vibration," *Physical Review Fluids,* vol. 9, no. 7, 73901, Jul 2024.

[21] E. D. Gedikli, J. M. Dahl, and D. Chelidze, "Multivariate analysis of vortex-induced vibrations in a tensioned cylinder reveal nonlinear modal interactions," *Procedia Engineering*, vol. 199, pp. 546-551, 2017.

[22] E. Aktosun, E. D. Gedikli, and J. M. Dahl, "Observed wake branches from the 2-DOF forced motion of a circular cylinder in a free stream," *Journal of Fluids and Structures,* vol. 124, 104035, Jan 2024.

[23] E. Aktosun, and E. D. Gedikli, "Modal decomposition analysis of two-degree-of-freedom vortex-induced vibrations," *Paper presented at the The 34th International Ocean and Polar Engineering Conference,* Rhodes, Greece, Jun 2024.

[24] E. Aktosun, "Investigation of Vortex-Induced Vibration of a Cylinder by Employing Cross-Flow and In-Line Motion," University of Rhode Island, 2020.

[25] E. Aktosun, "Modeling fluid forces in 2-DOF forced motion experiments using neural network and analytical nonlinear approaches," *Ocean Engineering*, vol. 330, 121231, Jun 2025.

[26] A. Khalak, and C. H. . Williamson, "Motions, forces and mode transitions in vortex-induced vibrations at low mass-damping," *Journal of Fluids and Structures,* vol. 13, no. 7-8, pp. 813-851, Oct 1999.

[27] T. Sarpkaya, "A critical review of the intrinsic nature of vortex-induced vibrations," *Journal of Fluids and Structures,* vol. 19, no. 4, pp. 389-447, May 2004.

[28] R. Gopalkrishnan, "Vortex-induced forces on oscillating bluff cylinders," Massachusetts Institute of Technology, 1993.

[29] J. J. M. Dahl, "Vortex-induced vibration of a circular cylinder with combined in-line and cross-flow motion," Massachusetts Institute of Technology, 2008. [Online]. Available: https://dspace.mit.edu/handle/1721.1/44747

[30] M. Rajabi, B. Mingels, E. Aktosun, J. Dahl, and E. Gedikli, "New insights into complex vortex-induced vibrations through 3d modeling and wake response analysis," *Bulletin of the American Physical Society*, Nov 2023.

[31] B. Mingels, J. Dahl, M. Rajabi, E. Gedikli, and E. Aktosun, "Evaluating 2D and 3D VIV wake modes and forces through forced motion simulations," *Bulletin of the American Physical Society,* Nov 2023.

[32] M. Rajabi, E. Aktosun, B. Mingels, J. Dahl, and E. D. Gedikli, "2D numerical forced-motion simulations of vortex-induced vibration wakes: Toward understanding the onset of three-dimensional effects," in *4th International Naval Architecture and Maritime Symposium*, 2023.

[33] B. Mingels, E. Aktosun, and J. Dahl, "Verification of wake branch response regions observed in 2-DOF forced motion of a circular cylinder," in *APS Division of Fluid Dynamics Meeting Abstracts*, 2024, pp. X38--003.

[34] N. I. Xiros and E. Aktosun, "Stabilization of neural network models for VIV force data using decoupled, linear feedback," *Journal of Marine Science and Engineering,* vol. 10, no. 2, 272, Feb 2022.

[35] P. J. Schmid, "Dynamic mode decomposition and its variants," *Annual Review of Fluid Mechanics,* vol. 54, no. 1, pp. 225-254, Jan 2022.

[36] D. Chelidze, "Higher-order decompositions for modal identification and model order reduction," in *Nonlinear Structures & Systems, Volume 1: Proceedings of the 38th IMAC, A Conference and Exposition on Structural Dynamics 2020*, 2020, pp. 271-278.